



ELSEVIER

Available online at [www.sciencedirect.com](http://www.sciencedirect.com)

SCIENCE @ DIRECT®

Progress in Biophysics and Molecular Biology 90 (2006) 207–224

Progress in  
Biophysics  
& Molecular  
Biology

[www.elsevier.com/locate/pbiomolbio](http://www.elsevier.com/locate/pbiomolbio)

## Review

# Spatial aspects of intracellular pH regulation in heart muscle

Richard D. Vaughan-Jones<sup>a,\*</sup>, Kenneth W. Spitzer<sup>b</sup>, Pawel Swietach<sup>a</sup>

<sup>a</sup>*Burdon Sanderson Cardiac Science Centre, University Laboratory of Physiology, Parks Road, Oxford, UK*

<sup>b</sup>*Nora Eccles Harrison Cardiovascular Research and Training Institute, University of Utah, Salt Lake City, USA*

Available online 7 July 2005

### Abstract

Intracellular pH ( $\text{pH}_i$ ) is an important modulator of cardiac function. Because it is readily influenced by metabolic processes,  $\text{pH}_i$  is controlled physiologically. Classical models of intracellular pH regulation comprise acid/base transport proteins expressed in the sarcolemma, acting in concert with intracellular buffers. These two processes are coupled via a diffusive movement of protons. Because intracellular  $\text{H}^+$  buffering is high,  $\text{H}_i^+$ -diffusion occurs through a passive shuttling on intrinsic mobile buffers such as acetylated carnosine, anserine and homocarnosine: low molecular weight imidazole compounds. This mechanism is assisted by carbonic buffer, a system regulated biochemically by the enzyme carbonic anhydrase.  $\text{H}_i^+$ -mobility via the buffer shuttles is low, and this can result in significant  $\text{pH}_i$  non-uniformity under conditions of high proton flux across the sarcolemma or within the cell. Spatial regulation of  $\text{pH}_i$  is complemented by passive  $\text{H}^+$  permeation between cells through gap junctions. This permeation is also mediated via protonated buffers. The control of  $\text{pH}_i$  is therefore dependent on carrier molecules that spatially shuttle protons within and between cells. In this review, we consider the physiological regulation of  $\text{H}_i^+$ -mobility and permeation, and its relevance to  $\text{pH}_i$ -control in normal and pathophysiological states such as myocardial ischaemia, a clinical condition associated with severe intracellular acidosis.

© 2005 Elsevier Ltd. All rights reserved.

### Contents

1. Introduction to intracellular pH regulation . . . . .	208
1.1. Functional importance of $\text{pH}_i$ . . . . .	208
1.2. Sarcolemmal control of $\text{pH}_i$ . . . . .	208
1.3. Coupling of cytoplasmic pH to sarcolemmal transporters . . . . .	209

\*Corresponding author.

0079-6107/\$ - see front matter © 2005 Elsevier Ltd. All rights reserved.

doi:10.1016/j.pbiomolbio.2005.06.004

2.	Regulation of intracellular proton mobility . . . . .	211
2.1.	Measuring $H_i^+$ mobility . . . . .	211
2.2.	Relationship between $D_H^{app}$ and intracellular buffering . . . . .	211
2.3.	Role of carbonic buffer. . . . .	213
3.	Spatial regulation of $pH_i$ within individual cells . . . . .	214
3.1.	Localised exposure to membrane permeant weak acids or bases . . . . .	214
3.2.	Stimulation of sarcolemmal acid efflux. . . . .	216
4.	Spatial regulation of $pH_i$ in cardiac cell-pairs. . . . .	218
4.1.	Protons permeate the gap junction. . . . .	218
4.2.	Mechanism of proton permeation . . . . .	219
4.3.	Local regulation of $pH_i$ via gap junctions. . . . .	220
5.	Conclusions. . . . .	221
5.1.	Spatial control of $pH_i$ . . . . .	221
5.2.	Spatial control via gap junctions . . . . .	221
5.3.	Possibility of spatial control during myocardial ischaemia . . . . .	221
	Editor's note . . . . .	222
	Acknowledgements. . . . .	222
	References . . . . .	222

## 1. Introduction to intracellular pH regulation

### 1.1. Functional importance of $pH_i$

Intracellular pH is an important modulator of cardiac function, influencing processes as varied as contraction (Bountra and Vaughan-Jones, 1989; Harrison et al., 1992), excitation and electrical arrhythmia (Orchard and Cingolani, 1994). Protons are produced metabolically within the heart, they are highly reactive with cellular proteins, and they must be removed if cardiac function is to be maintained. A sophisticated system for regulating  $pH_i$  has therefore evolved in heart cells. Steady-state  $pH_i$  is typically 7.1–7.3 (Leem et al., 1999; Yamamoto et al., 2005). It can decline modestly with an increase in heart rate (Bountra et al., 1988; Elliott et al., 1994) and, more dramatically, during myocardial ischaemia (Garlick et al., 1979) where it accounts for much of the observed failure of contraction (Katz and Hecht, 1969). Intracellular pH will also be influenced by extrinsic events such as changes in whole body acid/base status.

### 1.2. Sarcolemmal control of $pH_i$

Acute displacement of  $pH_i$  from its steady-state level is compensated for within minutes by means of sarcolemmal acid or base extrusion on ion-coupled transport proteins (Leem et al., 1999). The functional arrangement of the transporters is illustrated schematically in Fig. 1A. Two types of transporter ( $Na^+ - H^+$  exchange: NHE, and  $Na^+ - HCO_3^-$  co-transport: NBC) mediate acid-extrusion while a further two ( $Cl^- - HCO_3^-$  exchange: AE, and  $Cl^- - OH^-$  exchange: CHE) mediate base extrusion. A fifth type of transporter shuttles lactic acid either into or out of the cell, during periods of high glycolytic flux (Poole et al., 1989). With the possible exception of the lactic acid carrier, kinetic activity of the transporters appears to be regulated allosterically by protons. An  $H^+$ -titratable site (or sites) on the protein senses the pH of the extracellular and intracellular compartments (cf. Stewart et al., 2004), and adjusts translocation of acid or base accordingly. This

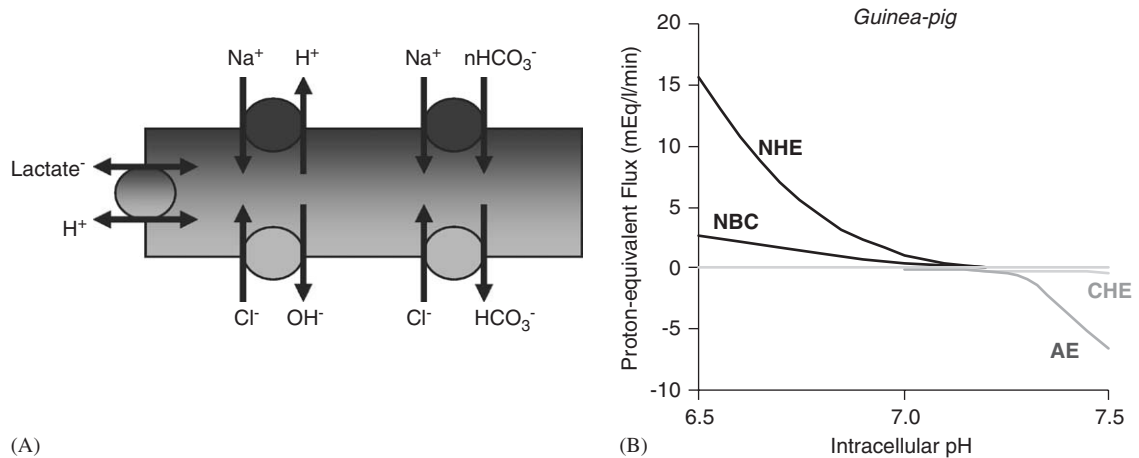


Fig. 1. Sarcolemmal  $\text{pH}_i$ -regulating mechanisms. (A) Five types of sarcolemmal protein have been shown to regulate intracellular  $\text{pH}_i$ .  $\text{Na}^+$ - $\text{H}^+$  exchange (NHE) and  $\text{Na}^+$ - $n\text{HCO}_3^-$  co-transport (NBC) are acid-extruders, activated strongly by a fall in  $\text{pH}_i$ .  $\text{Cl}^-$ - $\text{OH}^-$  exchange (CHE) and  $\text{Cl}^-$ - $\text{HCO}_3^-$  exchange (AE) are acid-loaders, activated by intracellular alkalosis. The monocarboxylic acid transporter (MCT) that co-transport lactate with protons can be an acid-loader or extruder, depending on transmembrane gradients of the substrates. B. Fluxes calculated for NHE, NBC, AE and CHE plotted as a function of intracellular  $\text{pH}$ , obtained from Leem et al. (1999). Near to resting  $\text{pH}_i$  ( $\text{pH}_i$  6.9–7.2) flux rates are low and give rise to a ‘permissive range’ where small deviations of  $\text{pH}_i$  are countered by only a small transmembrane acid-flux.

ensures the regulation of  $\text{pH}_i$ . Kinetic control of the four principal  $\text{pH}$ -regulatory transporters by intracellular  $\text{pH}$  is illustrated in Fig. 1B. Note that acid extrusion is stimulated by intracellular acidosis while base extrusion is stimulated by alkalosis, but that all four transporters display low levels of activity when  $\text{pH}_i$  is close to 7.1, the steady-state value.

The model of  $\text{pH}_i$  regulation presented in Fig. 1 has been useful in the development of computational algorithms for  $\text{pH}_i$  regulation (Leem et al., 1999), coupled to cellular models of cardiac excitation and contraction (Ch'en et al., 1998). This has permitted functional responses to an acid/base disturbance to be simulated with a reasonable degree of accuracy. Such models are proving useful in elucidating the role of  $\text{pH}$ -transporters in the triggering of arrhythmia and contractile dysfunction during clinical conditions such as myocardial ischaemia and reperfusion, which are associated with large excursions of  $\text{pH}_i$ .

### 1.3. Coupling of cytoplasmic $\text{pH}$ to sarcolemmal transporters

The model in Fig. 1 suffers from the major disadvantage of not providing information on the cytoplasmic distribution of  $\text{H}^+$  ions. In order for transport at the sarcolemma to regulate bulk cytoplasmic  $\text{pH}$ , the two domains must be coupled functionally. This is achieved by the spatial diffusion of intracellular acid. For example, stimulation of acid extrusion across the surface membrane depletes sub-sarcolemmal  $[\text{H}^+]_i$  which then induces a diffusive influx of protons into the microdomain from the surrounding cytoplasm, thus raising bulk cytoplasmic  $\text{pH}$  (see Swietach and Vaughan-Jones, 2005a). There is a problem, however, with the implementation of

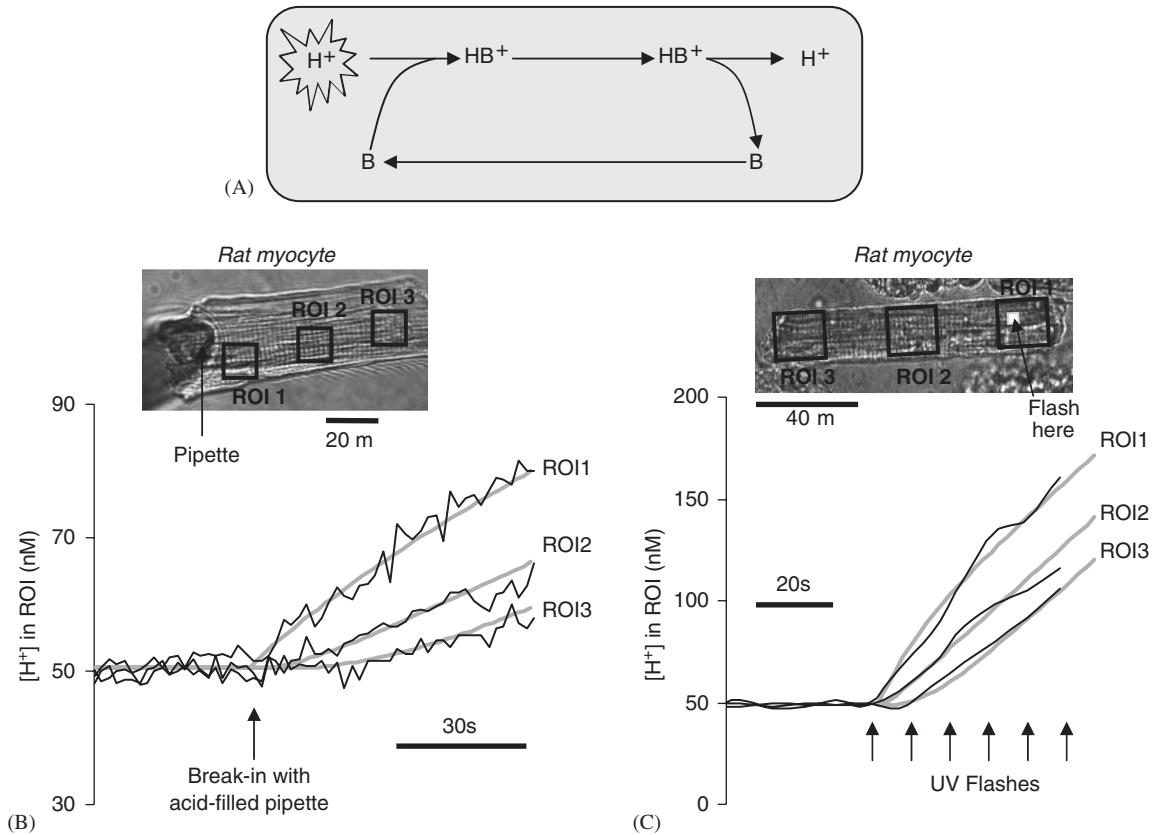


Fig. 2. Measuring intracellular proton mobility in cardiac myocytes. (A) A local acid disturbance can be dissipated within cytoplasm by mobile buffer, B. Protonated buffer, HB<sup>+</sup>, carries the excess acid to regions of higher pH. (B) Effect of a local pH<sub>i</sub> disturbance, produced in a rat ventricular myocyte by injection of acid through a cell-attached micropipette filled with unbuffered, isotonic KCl plus 1 mM HCl. The progress of acid-loading in three downstream regions of interest (ROI) in the cell (see inset) is fitted with diffusion equations, giving a best-fitting apparent diffusion coefficient ( $D_{\text{H}}^{\text{app}}$ ) of  $2.5 \times 10^{-7} \text{ cm}^2/\text{s}$ . Modified from Zaniboni et al., 2003b. (C) Continuous acid-loading can be approximated by a 0.11 Hz sequence of brief (9.8  $\mu\text{s}/\text{pixel}$ ) flashes of UV light in a small ROI positioned within the outline of a rat ventricular myocyte, superfused with the caged proton compound, 1 mM 2-nitrobenzaldehyde (NBA). The continuous curves depict the acid-loading time-courses with a best-fitting  $D_{\text{H}}^{\text{app}}$  of  $11 \times 10^{-7} \text{ cm}^2/\text{s}$  (Swietach et al., 2005b). Results in both (B) and (C) are consistent with a low intracellular proton mobility.

this process. Owing to the high buffering capacity of cytoplasmic proteins, spatial diffusion of H<sub>i</sub><sup>+</sup> may be extremely slow (any diffusing H<sup>+</sup> ions will be captured on fixed buffer sites), thereby decoupling cytoplasmic pH from the sarcolemmal control sites. The problem is solved by the provision of intracellular mobile buffers. These are molecules of relatively low molecular weight (100–200 Da), which diffuse two or three orders of magnitude faster than large proteins. They reversibly bind and shuttle protons spatially within the cell, as illustrated schematically in Fig. 2A. Thus, although intracellular H<sup>+</sup> ion flux is low under most physiological conditions, mobile buffers can provide significant spatial movement of acid, thus restoring the coupling between cytoplasmic pH and the sarcolemmal pH regulatory transporters. The efficiency of this coupling

will determine the size and longevity of spatial  $\text{pH}_i$  gradients induced by membrane transport or local acid/base disturbances. An understanding of  $\text{pH}_i$  regulation therefore requires elucidation of its spatial properties.

## 2. Regulation of intracellular proton mobility

### 2.1. Measuring $\text{H}_i^+$ mobility

Intracellular proton mobility has recently been measured experimentally in enzymically isolated ventricular myocytes (Vaughan-Jones et al., 2002; Zaniboni et al., 2003a, b; Swietach et al., 2005b). In order to do this,  $\text{pH}_i$  was displaced locally within a cell, and confocal  $\text{pH}_i$ -imaging applied to determine its spatiotemporal behaviour. This is illustrated in Figs. 2B and C, which show two different experimental approaches. In panel B, a myocyte was loaded locally with acid from a cell-attached glass micropipette filled with isotonic KCl solution at pH 3.0 (i.e. containing 1 mM HCl). The rise of  $[\text{H}^+]_i$  in three regions downstream from the pipette was monitored. Acidification in the most distal region lagged that in the proximal region by 30–40 s, indicating a very slow movement of acid down the length of the cell. The continuous lines were best-fitted to the regional time-courses using equations for diffusion from a constant point-source into a compartment defined by the 2D outline of the cell (see inset). The best-fitting value for the apparent proton diffusion coefficient,  $D_{\text{H}}^{\text{app}}$ , was  $2.5 \times 10^{-7} \text{ cm}^2/\text{s}$ . A value for  $D_{\text{H}}^{\text{app}}$  of  $11 \times 10^{-7} \text{ cm}^2/\text{s}$  was deduced in a cell where acid was loaded locally by photolytically uncaging it from the intracellular proton-donor, 1 mM 2-nitrobenzaldehyde (NBA), using repetitive ( $\sim 0.1$  Hz) localised flashes (9.8  $\mu\text{s}/\text{pixel}$ ) from an ultra-violet laser, as shown in panel C. On average, using the pipette-loading technique, the value of  $D_{\text{H}}^{\text{app}}$  calculated for rat, rabbit and guinea-pig ventricular myocytes ranges from  $4 \times 10^{-7}$  to  $12 \times 10^{-7} \text{ cm}^2/\text{s}$  (Vaughan-Jones et al., 2002; Zaniboni et al., 2003b). These values for  $D_{\text{H}}^{\text{app}}$  are two orders of magnitude lower than for protons in pure water ( $D_{\text{H}} = 1.2 \times 10^{-4} \text{ cm}^2/\text{s}$ , Vanysek, 1999) emphasising that, even in the presence of intracellular mobile buffers,  $\text{H}_i^+$  mobility is greatly impeded.

### 2.2. Relationship between $D_{\text{H}}^{\text{app}}$ and intracellular buffering

A theoretical treatment of the buffer hypothesis of  $\text{H}_i^+$  mobility (Junge and McLaughlin, 1987; Irving et al., 1990; Swietach et al., 2003) predicts that, at a given  $\text{pH}_i$ ,  $D_{\text{H}}^{\text{app}}$  is determined by (i) the diffusion coefficient of the mobile buffer ( $D_{\text{mob}}$ , for simplicity this can be lumped for all intracellular mobile buffers and assumed to be  $\text{pH}_i$ -independent) and (ii) the fraction of the intracellular buffer capacity that is mobile.  $D_{\text{H}}^{\text{app}}$  can be approximated by the equation

$$D_{\text{H}}^{\text{app}} = D_{\text{mob}} \frac{\beta_{\text{mob}}}{\beta_{\text{tot}}}, \quad (1)$$

where  $\beta_{\text{mob}}$  is the buffer capacity summed for all mobile buffers, and  $\beta_{\text{tot}}$  is total buffer capacity (buffering is expressed as the concentration of acid-equivalents, mmoles/litre of cytoplasm, required to change  $\text{pH}_i$  by one unit). The latter term represents the mobile buffer capacity *plus* that summed for all fixed (or very poorly mobile) buffers, such as cytoplasmic proteins. Intrinsic

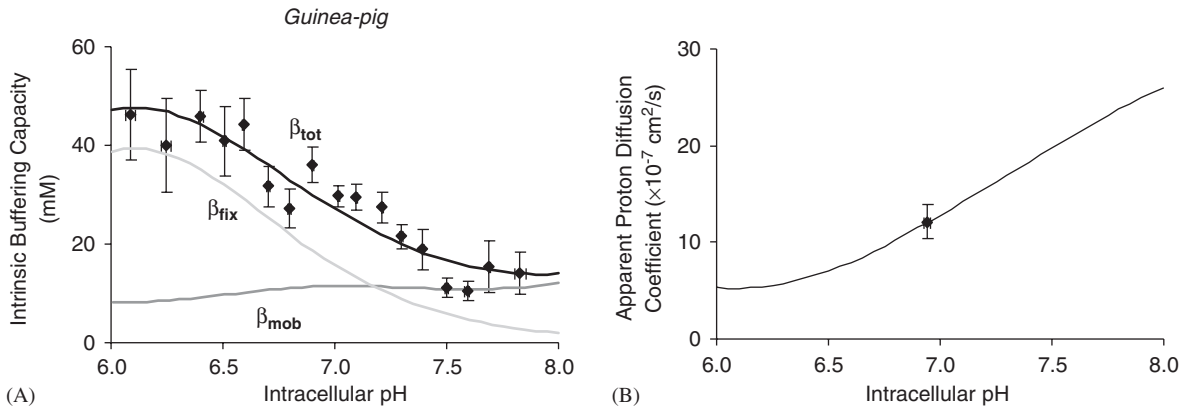


Fig. 3. Mobile and fixed buffering capacity determine intracellular proton mobility. (A) Experimental data for total intrinsic buffering capacity,  $\beta_{tot}$ , were derived using the ammonium-removal method (data from Zaniboni et al., 2003b). The mobile buffering capacity,  $\beta_{mob}$ , was estimated from biochemical data on putative intracellular mobile buffers (Vaughan-Jones et al., 2002). The difference between total buffering capacity and mobile buffering capacity was taken as the fixed buffering capacity,  $\beta_{fix}$ . (B) By calculating the mobile-to-total buffering capacity ratio from (A) and using a value of  $D_{mob}$  derived from the  $\text{pH}_i$ - $D_H^{app}$  relationship obtained experimentally, it was possible to predict the  $\text{pH}_i$ -dependence of intracellular proton mobility (modified from Zaniboni et al., 2003b). Experimental data for  $D_H^{app}$  ( $n = 20 \pm \text{SEM}$ ) measured by Zaniboni et al. (2003a, b) are included as a test of the model (filled symbol).

mobile buffers are likely to be, principally, acetyl anserine, acetyl carnosine and homocarnosine, all of which are present at relatively high concentration in cardiac and skeletal muscle cells (combined concentration in cardiac cells is about 18 mM, O'Dowd et al., 1988). These compounds are dipeptides that contain an imidazole group. Most fixed buffering is also likely to be via imidazole groups but, in this case, they are integrated within cytoplasmic proteins. Other molecules such as inorganic phosphate, intracellular taurine and cytoplasmic amino acids may contribute to mobile buffering but, at resting  $\text{pH}_i$  and under normal physiological conditions, these latter contributions will be small (see Table 1 of Vaughan-Jones et al., 2002, for a listing of intracellular mobile buffers).

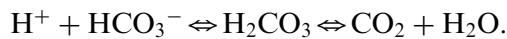
Recent analyses of total intrinsic buffering capacity ( $\beta_{tot}$ ) in rat, rabbit and guinea-pig ventricular myocytes suggest that it varies with  $\text{pH}_i$  in a manner consistent with at least two populations of buffer (see Fig. 3A), one of high concentration ( $\sim 70$  mM) and low average  $\text{pK}$  ( $\sim 6.1$ ) and one of lower concentration ( $\sim 15$  mM) comprising a broader range of  $\text{pK}$  values (Zaniboni et al., 2003b). If one assumes that the low  $\text{pK}$  population provides fixed buffering while the other population provides mobile buffering, then the observed spatiotemporal behaviour of intracellular pH during or after its local displacement can be readily simulated by using diffusion equations to predict the movement of mobile buffer (Swietach et al., 2003, 2005a).

Inspection of Fig. 3A suggests that the fraction of total intracellular buffering that is mobile should decrease with  $\text{pH}_i$  over the range from 8.0 to 6.0. Assuming that the diffusion coefficient for mobile buffer ( $D_{mob}$ ) is unaffected by this change of  $\text{pH}_i$ , Eq. (1) predicts that  $\text{H}_i^+$  mobility (i.e.  $D_H^{app}$ ) in the ventricular myocyte should decline with  $\text{pH}_i$ , (Fig. 3B). Indeed, in axoplasm extruded from a molluscan nerve,  $D_H^{app}$  appears to decrease at low  $\text{pH}_i$ , but this result has little

bearing on mammalian heart cells, as intracellular mobile and fixed buffers may be radically different in the two cases (Al-Baldawi and Abercrombie, 1992). Nevertheless, recent measurements of  $D_{\text{H}}^{\text{app}}$  at different  $\text{pH}_i$  values in rat and guinea pig ventricular myocytes have shown that such a decline can also be measured (Swietach and Vaughan-Jones, 2005b). Thus the diffusive coupling of bulk cytoplasmic pH to sarcolemmal acid transport is likely to be weakened during an intracellular acid-load.

### 2.3. Role of carbonic buffer

An important intracellular and extracellular buffer is the  $\text{CO}_2/\text{HCO}_3^-$  system. For convenience, we define this as carbonic buffer. Buffering occurs via the reversible protonation of bicarbonate anions leading to the release of  $\text{CO}_2$ ,



Carbonic buffering is powerful provided (i) the surface membrane is highly permeable to  $\text{CO}_2$  (so that fluctuations of intracellular  $\text{CO}_2$  can be damped via membrane permeation) and (ii) the partial pressure of extracellular  $\text{CO}_2$  is maintained relatively constant (through ventilation at the lungs).  $\text{CO}_2$  readily permeates the sarcolemma, and extracellular  $[\text{CO}_2]$  is usually well controlled in the heart as long as vascular perfusion is adequate. Both conditions are therefore met in the healthy myocardium. As both  $\text{CO}_2$  and  $\text{HCO}_3^-$  are low molecular weight solutes they will have high intracellular mobility (Swietach et al., 2003). Carbonic buffer may therefore be expected to shuttle protons spatially within the cell, as illustrated in Fig. 4.

Experimental measurements of  $\text{H}_i^+$  mobility have indicated that the presence of 5%  $\text{CO}_2/23\text{ mM HCO}_3^-$  enhances  $\text{H}_i^+$  mobility by 2–5-fold (Stewart et al., 1999; Spitzer et al., 2002; Zaniboni et al., 2003b), consistent with proton movement via the carbonic shuttle. This level of enhancement, however, requires the activity of the enzyme, carbonic anhydrase (CA), which catalyses the reversible hydration of  $\text{CO}_2$ . Inhibition of CA with acetazolamide attenuates the enhancement, indicating that the rate of proton shuttling is likely to be limited by the chemical hydration of  $\text{CO}_2$  (Stewart et al., 1999; Spitzer et al., 2002). CA is known to be expressed in cardiac cells although its functional activity is relatively modest. In guinea-pig ventricular myocytes, CA catalyses the rate of  $\text{CO}_2$ -hydration by 2.6-fold (Leem and Vaughan-Jones, 1998).

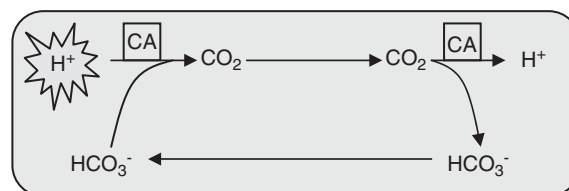


Fig. 4. Carbonic buffer plays a role in providing additional mobile buffer for facilitating intracellular proton flux. The ability of carbonic buffer to shuttle protons inside cells depends on the availability of the open, membrane-permeant form of the buffer ( $\text{CO}_2$ ) from the extracellular medium, and on the speed of hydration of  $\text{CO}_2$  to carbonic acid, and back. The former is not a limiting factor, because membranes are highly permeable to  $\text{CO}_2$ , whereas the latter factor is slow. Carbonic anhydrase (CA) accelerates intracellular  $\text{H}^+$  mobility by 3-fold in guinea-pig myocytes (Zaniboni et al., 2003b).

The regulation of  $H_i^+$ -mobility by CA is physiologically important, as an increase in  $D_H^{app}$  will help to minimise the development of  $pH_i$  gradients, thus maintaining a spatially homogeneous  $pH_i$ . The relatively slow hydration of  $CO_2$ , even in the presence of active CA means, however, that the carbonic shuttle can minimise spatial  $pH_i$  gradients only when they are generated by a low rate of local acid production within the cell. Recent work has shown that when local acid-production is high as occurs, for example, during partial exposure of a cell to membrane permeant weak acid or base (see next section), the carbonic-shuttle collapses  $pH_i$  gradients by no more than about 10% (Swietach et al., 2005a). Under these circumstances considerable  $pH_i$  heterogeneity may therefore occur.

The site of CA that enhances  $H_i^+$ -mobility is unknown. Soluble cytoplasmic CA has not been detected in cardiac tissue (Vandenberg et al., 1996) while one, possibly two, membrane-bound CA isoforms have been reported (Sender et al., 1998; Knuppel-Ruppert et al., 2000). These, however, have been proposed to be exofacial, associated partly with  $pH_i$  regulatory transporters such as NBC (Loiselle et al., 2004) and AE (Sterling et al., 2002). Another site for cardiac CA is believed to be on the luminal face of the sarcoplasmic reticular membrane. While it is conceivable that such sites may catalyse cytoplasmic  $H_i^+$ -mobility (given that  $CO_2$  is membrane permeant), an alternative explanation is that the active sites of some membrane-located CA proteins are exposed to the cytoplasmic compartment.

### 3. Spatial regulation of $pH_i$ within individual cells

Given that many spatially distributed proteins in the cardiac myocyte display pH-sensitivity over the physiological pH-range, a severe heterogeneity of  $pH_i$  will result in differential modulation of these proteins in different regions of the cell. For example, contractile protein interactions will be reduced by an acidosis acting directly at the cross-bridge (see Orchard and Kentish, 1990, for a review), and indirectly by competing with  $Ca^{2+}$  for binding to troponin C (Fabiato and Fabiato, 1978). Any  $pH_i$  heterogeneity will therefore regionally affect myofibrillar activity. This may compromise the smooth progression of the contractile cycle. It seems reasonable to suppose that the control of  $H_i^+$ -mobility by intracellular mobile buffers is geared towards attenuating any  $pH_i$  non-uniformity. Nevertheless, intracellular proton mobility is remarkably low, and so under some circumstances, significant  $pH_i$  gradients are likely to occur. We consider two such circumstances.

#### 3.1. Localised exposure to membrane permeant weak acids or bases

Fig. 5 shows an experiment where an isolated guinea-pig ventricular myocyte was superfused with solutions from a double-barrelled micropipette. The boundary between the two microstreams was directed at right angles to the long axis of the cell. In this way each end of the cell could be exposed to a different solution. In Fig. 5A, the right hand side of the cell was exposed to Tyrode solution containing 20%  $CO_2$  and 88 mM  $HCO_3^-$  (osmotically balanced) while the left hand side was exposed to nominally  $CO_2$ -free HEPES-buffered Tyrode. Local entry of  $CO_2$  into the right end acidified that region while  $pH_i$  at the left end remained virtually unaffected. A large longitudinal  $pH_i$  gradient of about 0.6 units was thus generated (Fig. 5B and C). The gradient stabilised within

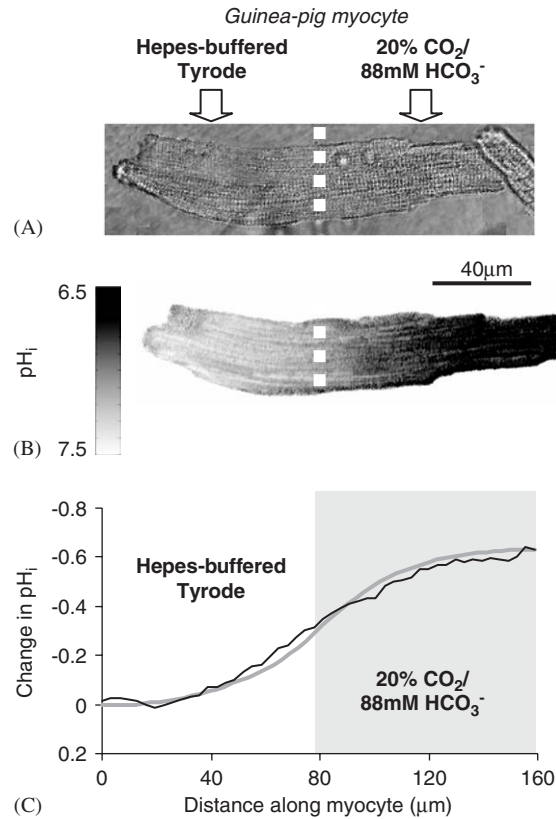


Fig. 5. Partial exposure of myocytes to CO<sub>2</sub> produces considerable intracellular pH non-uniformity. (A) Myocytes can be dually superfused with microstreams emerging from a double barrelled micropipette (direction of flow indicated by the open arrows). The degree of mixing at the boundary between the solutions is minimal due to high flow rates. (B) Upon exposing the right end of the guinea-pig myocyte to 20% CO<sub>2</sub>, within 30 s, a large and stable end-to-end pH<sub>i</sub> gradient of 0.6 units was generated (myocyte AM-loaded with carboxy-SNARF-1). (C) The end-to-end gradient (black trace) could be reproduced (grey trace) using a diffusion-reaction model based on mobile and fixed buffers (see Swietach et al., 2005a, for further details).

about 30 s, and remained for as long as dual microperfusion was applied. Similar gradients can be generated by partly exposing a cell to salts of other membrane permeant weak acids such as propionic or acetic acid, or to salts of the weak base ammonia, which generates a local rise of pH<sub>i</sub> (Spitzer et al., 2000; Swietach et al., 2005a).

The grey line fitted to the longitudinal pH<sub>i</sub> gradient in Fig. 5C represents the prediction of a computational model (Swietach et al., 2005a) where proton mobility is simulated by the diffusion of intracellular mobile buffer (see Fig. 3A). The pH<sub>i</sub> gradient stabilises because acid-equivalent injection into the right end of the cell, induced by CO<sub>2</sub> entry, attains a steady state with CO<sub>2</sub> continuously venting from the left end of the cell. Within the cell, acid diffuses longitudinally, from a region of high to a region of low proton concentration. This acid movement is mediated through the intracellular buffer-shuttle (from right to left). In the steady state, the rate of longitudinal acid diffusion must match the rate of intracellular acid injection at the right end of

the cell, and the rate of acid efflux from the left end. Because  $H_i^+$  mobility is so low, a large  $pH_i$  gradient is required to drive the longitudinal acid flux at steady state. Exposure of a cell to an extracellular gradient of  $[CO_2]$  thus induces a large and stable  $pH_i$  non-uniformity that is a direct consequence of low  $H_i^+$ -mobility.

Although such spatial gradients of  $CO_2$  are unlikely to occur physiologically, they are known to occur under some clinical conditions, most notably at the border zones of regionally ischaemic areas in the myocardium (e.g. Cascio et al., 1992). Buffering of anaerobically generated lactic acid by intracellular bicarbonate produces a high  $[CO_2]$  in the ischaemic zone. Some  $CO_2$  may also be produced from anaerobic reactions in mitochondria, notably the decarboxylation of oxoglutarate (a by-product, under hypoxic conditions, of the conversion of pyruvate to alanine; Taegtmeyer, 1978). Local  $P_{CO_2}$  during ischaemia can be in excess of 200 mmHg, while it is normally about 40 mmHg beyond the border zone (Case et al., 1979; Cascio et al., 1992). While this large gradient of  $[CO_2]$  is unlikely to be spatially as steep as that imposed on the single cell illustrated in Fig. 5, some experimental models of regional ischaemia indicate that it may occur over a distance of only a few myocyte cell-lengths (e.g. Wilensky et al., 1986). The  $[CO_2]$  gradient would then be expected to induce large  $pH_i$  gradients both within a given myocyte (Spitzer et al., 2000; Swietach et al., 2005a) and within cell-pairs (Swietach and Vaughan-Jones, 2004) or clusters of myocytes at the border zone. The effect of such gradients on other cell parameters such as  $[Ca^{2+}]_i$  is not known, but it is of interest that  $pH_i$  and  $Ca_i^{2+}$  are functionally coupled in heart (Vaughan-Jones et al., 1983; Kohmoto et al., 1990). Furthermore, border zones of locally ischaemic or injured myocardial regions are reported to be sites of intracellular  $Ca^{2+}$  waves that may underlie local profiles of abnormal electrical activity (Tanaka et al., 2002; Tsujii et al., 2003). An intracellular  $pH$  gradient may therefore be one consequence of regional ischaemia. Spatial imaging of  $pH_i$  across ischaemic border zones will be required to test this possibility.

### 3.2. Stimulation of sarcolemmal acid efflux

One cause of  $pH_i$  non-uniformity will be sarcolemmal acid/base transport (Swietach and Vaughan-Jones, 2005a). The experiment shown in Fig. 6 explores whether physiologically significant  $pH_i$  gradients are generated when sarcolemmal acid extrusion is stimulated. A rat ventricular myocyte was acid-loaded by prepulsing it with 20 mM ammonium chloride in the absence of extracellular  $Na^+$ . Re-addition of  $Na^+$  to the bathing solution permitted the activation of acid extrusion on NHE. The time-course of whole-cell  $pH_i$ -recovery averaged for several experiments is shown in panel Ab. Panel Ac shows the  $pH_i$  at the end-regions of the cell relative to that measured in the middle. This has been estimated as the average  $pH$  difference,  $\Delta pH$ , in (ROI1–ROI2) and (ROI3–ROI2). If  $pH_i$  were spatially uniform during  $pH_i$  recovery, there would be no difference. It is apparent, however, that a difference of up to 0.1 units was generated transiently during the NHE activation, indicating that  $pH_i$ -recovery was fastest at the ends of the cell. Thus during stimulation of NHE, there was a biphasic spatial  $pH_i$  gradient, with the ends being more alkaline.

Once  $pH_i$ -recovery was complete, the longitudinal  $pH_i$  gradient subsided. The greater the initial acid load, the larger was the ensuing  $pH_i$  gradient (Fig. 6B), indicating that it was related to the magnitude of acid efflux, which is stimulated at low  $pH_i$ . Spatial  $pH$  analysis revealed that significant ( $>0.03$ ) radial  $pH$  gradients could not be detected during the experiment.

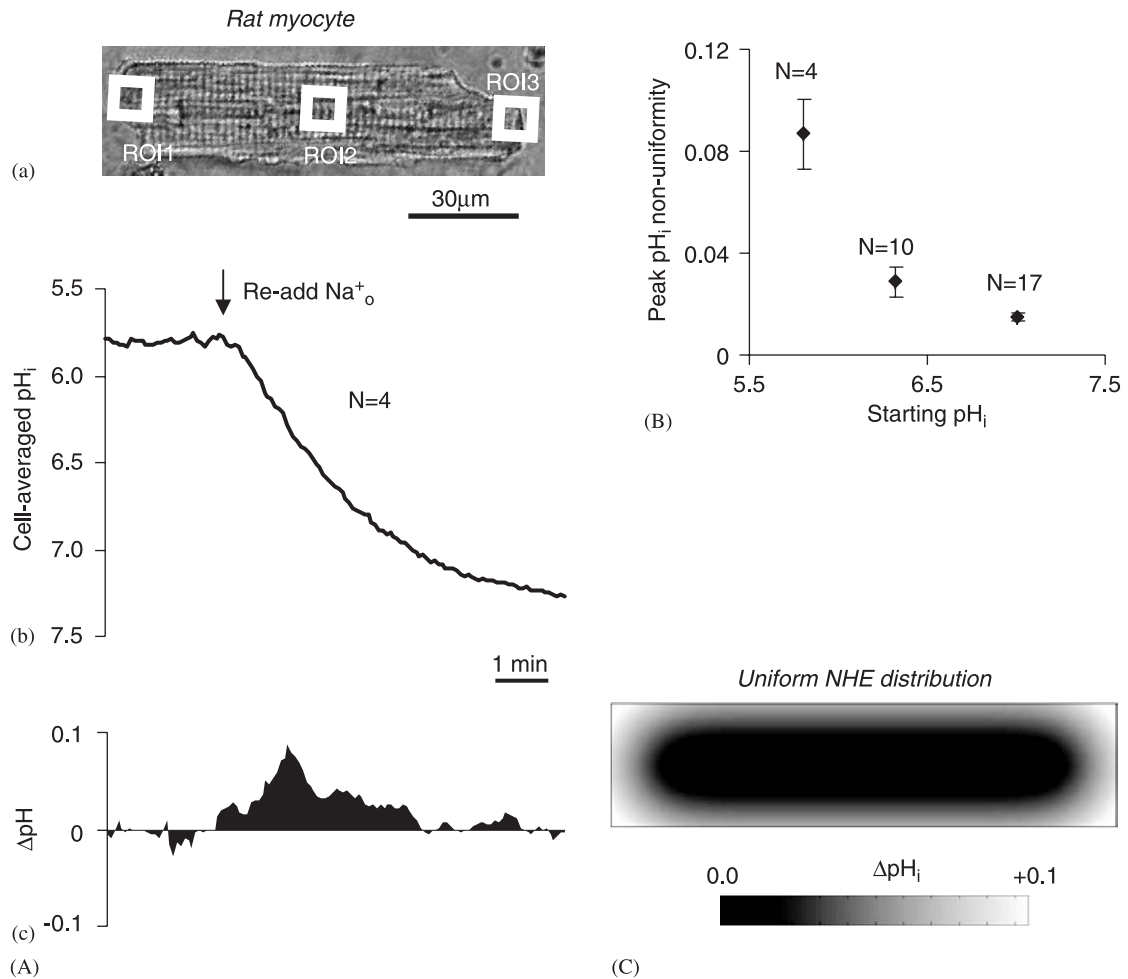


Fig. 6. Rapid activation of sarcolemmal pH transporters at low starting  $pH_i$  produces significant  $pH_i$  non-uniformity. Modified from Swietach and Vaughan-Jones (2005a). (A) A rat ventricular myocyte (Aa) was imaged confocally using the fluorescent dye, carboxy-SNARF-4F, in three ROIs before and after re-addition of  $Na^+$  to the superfusion medium (whole-cell  $pH_i$  recovery shown in Ab). The end-to-centre  $pH_i$  gradient (taken as the average of the pH difference in ROI1-ROI2 and ROI3-ROI2) shown in (Ac) suggests significant non-uniformity of up to 0.1 pH unit. (B) The size of the peak  $pH_i$  non-uniformity during acute NHE activation depends on the starting  $pH_i$ . Low  $pH_i$  provides favourable conditions for the development of  $pH_i$  non-uniformity as the proton mobility is low (Fig. 3B) and the activity of NHE is high (Fig. 1B). (C) A computational model of spatially distributed  $pH_i$ , determined at peak non-uniformity during acid extrusion from a compartment comparable in size to the ventricular myocyte (from Swietach and Vaughan-Jones, 2005a), again suggests significant non-uniformity.

A computational model with the cell considered to be cylindrical (Swietach and Vaughan-Jones, 2005a), was able to reproduce the spatial behaviour of  $pH_i$  (Fig. 6C) provided a low  $H_i^+$ -mobility was assumed (Fig. 3B). The model, however, required that NHE transporters be expressed uniformly at the ends as well as the sides of the cylinder, otherwise the longitudinal pH gradient was not predicted.

The experiment and modelling indicate that the size of acid efflux on a  $\text{pH}_i$ -regulatory transporter is not likely to generate significant radial  $\text{pH}_i$  gradients in a cardiac myocyte, despite the low  $\text{H}^+$ -mobility. The clear *longitudinal* gradient, however, was a surprise and demonstrates that efficient spatial coupling in the ventricular myocyte can be compromised at high sarcolemmal transport rates. A non-uniformity of up to 0.1 units would, for example, be expected to exert a regional influence on cell contraction. Whether such intracellular gradients occur in the intact myocardium cannot yet be answered. A high expression of NHE proteins has been reported previously at gap junctions (Petrecca et al., 1999), and the present work indicates that these transporters are functional. It is not known, however, whether they can extrude acid into the restricted cleft between adjacent cells at the intercalated disk. This may require a mechanism to facilitate the subsequent passage of acid into the bulk extracellular phase. The alternative possibility that end-NHE proteins normally mediate cell-to-cell passage of acid can be discounted as a selective NHE inhibitor, cariporide, does not affect intercellular acid transmission (Zaniboni et al., 2003a; see also next section). The physiological role of end-NHE transporters therefore remains to be established.

#### 4. Spatial regulation of $\text{pH}_i$ in cardiac cell-pairs

Individual cardiac cells possess the full apparatus for  $\text{pH}_i$  regulation, sited within localised regions of cytoplasm, and at the sarcolemma. Depending on species, the myocardium, however, consists of tens or even hundreds of millions of cardiac cells. The question is whether individual cells continue to function as independent  $\text{pH}$  regulators when amalgamated within the whole organ, or whether information pertinent to  $\text{pH}_i$  regulation is shared among cells, thus co-ordinating the myocardial response. A start to assessing this question can be made by exploring spatial  $\text{pH}_i$  control in couplets of ventricular myocytes isolated enzymically in the same way as for individual cells.

##### 4.1. Protons permeate the gap junction

Fig. 7A shows acid being locally diffused into one end of an end-to-end pair of cells via a cell-attached acid-filled micropipette. Sarcolemmal acid transporters were inhibited by applying cariporide (NHE inhibitor) and by using Hepes-buffered, nominally  $\text{CO}_2$ -free superfusates (to inhibit NBC). The cell pair had previously been loaded with the AM-ester of carboxy-SNARF-1 to permit confocal  $\text{pH}_i$  imaging. Regions close to the injection site acidified fastest, but it is evident that acid also percolated into the second, downstream cell, through the cell-cell junctional region. The continuous lines best-fitted to the regional  $\text{pH}_i$  time-courses were generated using 2D diffusion equations for protons, assuming a point source for acid injection, and assuming a single value for the apparent  $\text{H}^+$  ion diffusion coefficient,  $D_{\text{H}}^{\text{app}}$ , determined from the best-fitting procedure (Zaniboni et al., 2003a). The computational model also contained a function describing junctional  $\text{H}^+$ -permeation where cell-cell  $\text{H}^+$ -flux is driven by the transjunctional proton gradient ( $\Delta[\text{H}^+]$ ):

$$J_{\text{H}}^{\text{app}} = -P_{\text{H}}^{\text{app}} \cdot \Delta[\text{H}^+].$$

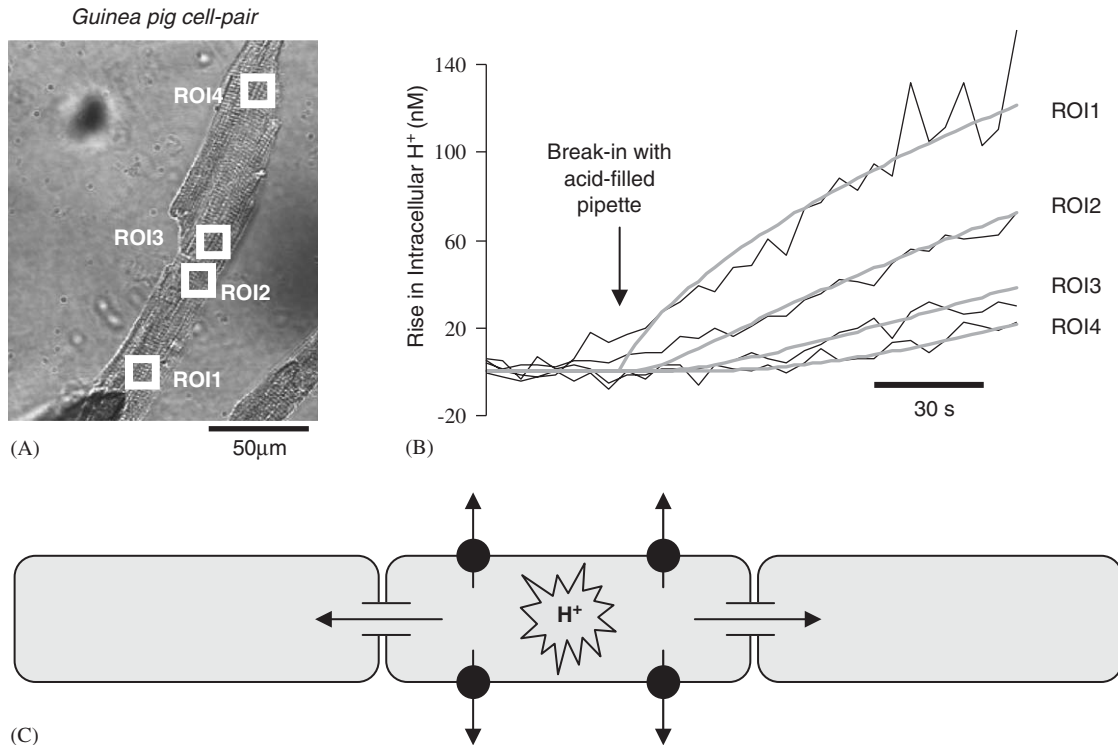


Fig. 7. Cell-to-cell acid transmission mediated by gap-junctions may serve a role in sharing  $pH_i$  information among myocardial cells. (A) An intact guinea-pig cell-pair was enzymically isolated from ventricle. (B) The cell-pair, loaded with the  $pH$  fluorophore carboxy-SNARF-1, was imaged confocally during a local injection of acid near ROI1 using an acid-filled micropipette (similar to Fig. 3C). The  $[H^+]$  time-courses (black traces) in the four ROIs were fitted with a diffusion model (grey traces) incorporating a permeation step at the cell-to-cell junction. Experiments like these have suggested an apparent proton permeation constant of  $2 \times 10^{-4}$  cm/s. Data in (A) and (B) taken from Zaniboni et al. (2003a). (C) Cell-to-cell proton flux is likely to be an important component of spatial  $pH_i$  regulation in multicellular preparations. For small localised  $pH_i$ -displacements, sarcolemmal transporters produce only a small acid efflux (Fig. 1B) yet, depending on the transjunctional gradient, intercellular proton flux may be considerable.

For simplicity, proton permeation is described by an apparent permeability constant ( $P_H^{app}$ ), which does not define the mechanism of proton transmission. A typical value for  $P_H^{app}$  is  $2 \times 10^{-4}$  cm/s (Zaniboni et al., 2003a). Similar values have also been deduced by partially exposing one cell of a cell-pair to weak acids or bases using dual microperfusion (as in Fig. 5;  $P_H^{app} = 4.5 \times 10^{-4}$  cm/s; Swietach and Vaughan-Jones, 2004) and in rat cell-pairs by photolytic uncaging of protons using flashes of UV-laser light (using the method shown in Fig. 2C;  $P_H^{app} = 4.9 \times 10^{-4}$  cm/s; Swietach et al., 2005b). Thus neighbouring cardiac cells can share  $pH_i$ -information across their gap-junctional regions.

#### 4.2. Mechanism of proton permeation

Cell-to-cell proton transmission is inhibited by pharmacological agents that inhibit gap-junctional conductance, namely  $\alpha$ - or  $\beta$ -glycyrrhetic acid (Zaniboni et al., 2003a). Such

conductance is due largely to expression of connexin 43 channels in ventricular gap-junctional regions (e.g. Yeager, 2000). Conversely, NHE proteins are unlikely to be involved, as the presence or absence of the NHE inhibitor, cariporide, has no effect on acid transmission (Zaniboni et al., 2003a). Thus cell-to-cell acid-transmission occurs via gap junctional channels.

The value for  $P_{\text{H}}^{\text{app}}$  at the gap junction is about 20-fold lower than that for another permeant solute, the  $\text{K}^+$  ion (Valiunas et al., 2002). As permeability of connexin channels to various solutes is determined largely by their size (although ionic charge can also play a role) this might imply, paradoxically, that permeating protons appear bigger than permeating  $\text{K}^+$  ions. Comparison with published permeability constants for molecules of various size suggests that protons permeate the cardiac gap junction as though they had a molecular mass of 100–200 Da (Swietach and Vaughan-Jones, 2004). Interestingly, this is the average molecular mass deduced previously for the intracellular mobile buffer molecules that shuttle protons within the cell (Vaughan-Jones et al., 2002). This raises the possibility that protons permeate gap junctions attached to permeant mobile buffers. This would then account for the fact that the permeating proton behaved as though it were a relatively large molecule. It would also mean that although free junctional  $\text{H}^+$  traffic appears small, as evidenced from imaging of free proton levels on either side of the junction, estimates of the total junctional proton flux could be reasonably high. This would be because almost all intercellular proton traffic is buffered, a situation exactly analogous to that for proton diffusion within cytoplasm. Interestingly, a theoretical consideration of the buffer model of cell–cell proton-transmission predicts a similar dependence of  $P_{\text{H}}^{\text{app}}$  on fractional mobile buffer capacity as derived previously for  $D_{\text{H}}^{\text{app}}$  (see Eq. (1)):

$$P_{\text{H}}^{\text{app}} = P_{\text{mob}} \frac{\beta_{\text{mob}}}{\beta_{\text{tot}}}, \quad (2)$$

where  $P_{\text{mob}}$  is the gap junctional permeability constant for permeant buffers. Given that molecules as large as 1 kDa can permeate cardiac gap junctions (Loewenstein, 1981), it is reasonable to assume that all intracellular mobile buffer is permeant. The model of proton permeation is therefore intriguing as it describes an ion (the  $\text{H}^+$  ion) moving through a channel (the connexin 43 channel) on a carrier (mobile buffer, dubbed a “proton porter”), a tantalising marriage of ion channel and ion carrier!

#### 4.3. Local regulation of $\text{pH}_i$ via gap junctions

Estimates of the total junctional cell-to-cell acid flux in experiments like that shown in Fig. 7B, indicate that it can be as large as typical estimates for sarcolemmal acid efflux on NHE during comparable intracellular acid loads (Zaniboni et al., 2003a). Thus dissipation of an acid-load through gap junctions will form one important means of locally controlling  $\text{pH}_i$ . This will supplement the more traditional sarcolemmal route for  $\text{pH}_i$  regulation. This dual approach to local  $\text{pH}_i$  regulation by gap junctions and by sarcolemmal transporters is summarised schematically in Fig. 7C. The model indicates that although cardiac myocytes can function as individual  $\text{pH}_i$  regulators, they will likely be co-ordinated by the sharing of  $\text{pH}_i$  information through their gap-junctions.

One important characteristic of gap junctions is not yet incorporated in the model shown in Fig. 7C, and that is their inhibitory gating by protons (Spray et al., 1981; Noma and Tsuboi, 1987; Delmar et al., 2000). The cell-to-cell flux of acid discussed above occurred during modest intracellular  $\text{pH}_i$  disturbances (where  $\text{pH}_i$  on one side of the junction was decreased to about

6.80). In cardiac cells, more severe acid-loads have been shown to reduce junctional conductance, most likely via a direct inhibitory effect of protons on the channel, and indirectly via secondary changes of  $\text{Ca}_i^{2+}$  induced by the initial intracellular acid load (Noma and Tsuboi, 1987; White et al., 1990). There is a real possibility, therefore, that junctional traffic of mobile buffer, and hence of acid, may be self-limiting, being truncated at lower  $\text{pH}_i$  values owing to proton-mediated closure of the “chemical gate” of the connexin channel. Experiments on the possible proton-gating of proton junctional flux are currently underway in our laboratory.

## 5. Conclusions

### 5.1. Spatial control of $\text{pH}_i$

The classical picture of  $\text{pH}_i$  regulation, where the sarcolemma is the key element, must now be revised to include the spatial architecture of the tissue, the spatial properties of intracellular proton diffusion, and intercellular proton permeation. Intracellular  $\text{H}^+$  mobility is physiologically regulated by the availability of titratable mobile buffer and fixed buffer, and this will be regulated by the ambient value of  $\text{pH}$  (given that buffer-capacity varies with  $\text{pH}$ ).  $\text{H}_i^+$  mobility is also enzymically regulated via the expression of the catalytic effect of CA on the hydration of  $\text{CO}_2$ , which forms an important part of the carbonic buffer shuttle.  $\text{H}_i^+$ -mobility mediated by the buffer shuttles is low, about two orders of magnitude lower than in water (Vaughan-Jones et al., 2002; Spitzer et al., 2002). This can sometimes lead to heterogeneity of  $\text{pH}_i$  within the cell, particularly when local rates of acid or base generation are high so that proton dissipation into adjacent cytoplasmic areas becomes rate-limiting. Intracellular proton mobility is an essential component of  $\text{pH}_i$  regulation as, without it, cytoplasmic  $\text{pH}$  would become uncoupled from the sarcolemma, effectively negating the ability of membrane transport to regulate  $\text{pH}_i$ .

### 5.2. Spatial control via gap junctions

Although proton-selective channels are not expressed in cardiac membranes, there is an important role for proton permeation through cardiac gap junctions. This is likely to assist in the local regulation of  $\text{pH}_i$ . It appears that the buffer shuttles that regulate  $\text{pH}_i$  spatially within the cell also extend through gap junctions to adjacent cells. This offers a novel form of spatial  $\text{pH}_i$  regulation not hitherto considered. Our knowledge about intercellular proton transmission, however, is currently limited to ventricular myocytes. It will be necessary to test for intercellular acid transmission between atrial, His bundle, Purkinje, and nodal cells (often involving different connexin (Cx) isoforms, in addition to Cx43), before applying the current model of spatial  $\text{pH}$  regulation to regions of the heart other than the ventricular myocardium.

### 5.3. Possibility of spatial control during myocardial ischaemia

One may speculate how spatial  $\text{pH}_i$ -regulation operates under pathophysiological conditions such as regional myocardial ischaemia. This disease is associated with localised pockets of acidosis within the myocardium. Within such zones, capillary perfusion is terminated, and so the only

routes for escape of acid into less acid-loaded regions are diffusive, through the extracellular and intracellular unstirred compartments. Gap junctions may therefore serve a useful role here in providing conduits for intracellular acid-dissipation into adjacent myocardium, especially as the classical sarcolemmal routes for acid efflux appear to be inactive during ischaemia (e.g. Allen and Xiao, 2003). The gap-junctional route will, however, be subject to modulation and gating by the acidosis itself, as well as by other factors presiding during the ischaemic episode. Without further experimental work, it would be premature to claim a major role for this pathway, but it is certainly an attractive possibility. Its role must be assessed at ischaemic border zones, where significant  $\text{pH}_i$  gradients may occur. Any link between non-uniformity of  $\text{pH}_i$  and abnormal  $\text{Ca}_i^{2+}$  signalling at these sites will be of considerable interest.

### Editor's note

Please see also related communications in this volume by Hervé and Sarrouilhe (2005) and Pelloux et al. (2005). For further downloadable content please see <http://www.physiome.org.nz/publications/PBMB-2005-89/Vaughan-Jones/>

### Acknowledgements

This work was supported by a programme grant from the British Heart Foundation (to RDVJ), a MERIT award from the National Heart, Lung and Blood Institute (to KWS; 5R37HL042873), a grant from the Nora Eccles Treadwell Foundation (to KWS), and a scholarship from the Wellcome Trust and Overseas Research Scheme (to PS). We thank Nurindura Banger (BHF Programme-funded) for excellent technical assistance.

### References

- Al-Baldawi, N.F., Abercrombie, R.F., 1992. Cytoplasmic hydrogen ion diffusion coefficient. *Biophys. J.* 61, 1470–1479.
- Allen, D.G., Xiao, X.H., 2003. Role of the cardiac  $\text{Na}^+/\text{H}^+$  exchanger during ischaemia and reperfusion. *Cardiovasc. Res.* 57 (4), 934–941.
- Boutra, C., Vaughan-Jones, R.D., 1989. Effect of intracellular and extracellular pH on contraction in isolated, mammalian cardiac muscle. *J. Physiol.* 418, 163–187.
- Boutra, C., Kaila, K., Vaughan-Jones, R.D., 1988. Effect of repetitive activity upon intracellular pH, sodium and contraction in sheep cardiac Purkinje fibres. *J. Physiol.* 398, 341–360.
- Cascio, W.E., Yan, G.X., Kleber, A.G., 1992. Early changes in extracellular potassium in ischaemic rabbit myocardium. The role of extracellular  $\text{CO}_2$  accumulation and diffusion. *Circ. Res.* 70, 409–422.
- Case, R.B., Felix, A., Castellana, F.S., 1979. Rate of rise of myocardial  $\text{PCO}_2$  during early myocardial ischemia in the dog. *Circ. Res.* 45, 324–330.
- Ch'en, F.F., Vaughan-Jones, R.D., Clarke, K., Noble, D., 1998. Modelling myocardial ischaemia and reperfusion. *Prog. Biophys. Mol. Biol.* 69 (2–3), 515–538.
- Delmar, M., Morley, G.E., Ek-Vitorin, J.F., Francis, D., Homma, N., Stergiopoulos, A.L., Taffet, S.M., 2000. Toward a molecular model for the pH regulation of intercellular communication in the heart. In: Zipes, D.P., Jalife, J.J. (Eds.), *Cardiac Electrophysiology from Cell to Bedside*. WB Saunders, London (Chapter 15).

- Elliott, A.C., Smith, G.L., Allen, D.G., 1994. The metabolic consequences of an increase in the frequency of stimulation in isolated ferret hearts. *J. Physiol.* 474, 147–159.
- Fabiato, A., Fabiato, F., 1978. Effects of pH on the myofilaments and sarcoplasmic reticulum of skinned cells from cardiac and skeletal muscles. *J. Physiol.* 276, 233–255.
- Garlick, P.B., Radda, G.K., Seeley, P.J., 1979. Studies of acidosis in the ischaemic heart by phosphorus nuclear magnetic resonance. *Biochem. J.* 184, 547–554.
- Harrison, S.M., Frampton, J.E., McCall, E., Boyett, M.R., Orchard, C.H., 1992. Contraction and intracellular  $\text{Ca}^{2+}$ ,  $\text{Na}^+$  and  $\text{H}^+$  during acidosis in rat ventricular myocytes. *Am. J. Physiol.* 262, C348–C357.
- Hervé, J.C., Sarrouilhe, D., 2005. Protein phosphatase modulation of the intercellular junctional communication: importance in cardiac myocytes. *Prog. Biophys. Mol. Biol.* 89.
- Irving, M., Maylie, J., Sizto, N.L., Chandler, W.K., 1990. Intracellular diffusion in the presence of mobile buffers. Application to proton movement in muscle. *Biophys. J.* 57, 717–721.
- Junge, W., McLaughlin, S., 1987. The role of fixed and mobile buffers in the kinetics of proton movement. *Biochim Biophys Acta* 890, 1–5.
- Katz, A.M., Hecht, H.H., 1969. The early pump failure of ischaemic heart. *Am. J. Med.* 47, 497–502.
- Knuppel-Ruppert, A.S., Gros, G., Harringer, W., Kubis, H.P., 2000. Immunochemical evidence for a unique GPI-anchored carbonic anhydrase isozyme in human cardiomyocytes. *Am. J. Physiol.* 278 (4), H1335–H1344.
- Kohmoto, O., Spitzer, K.W., Movsesian, M.A., Barry, W.H., 1990. Effects of intracellular acidosis on  $[\text{Ca}^{2+}]_i$  transients, transsarcolemmal  $\text{Ca}^{2+}$  fluxes, and contraction in ventricular myocytes. *Circ. Res.* 66 (3), 622–632.
- Leem, C.H., Vaughan-Jones, R.D., 1998. Out of Equilibrium pH transients in the guinea-pig ventricular myocyte. *J. Physiol.* 509, 471–485.
- Leem, C.H., Lagadic-Gossman, D., Vaughan-Jones, R.D., 1999. Characterisation of intracellular pH regulation in the guinea-pig ventricular myocyte. *J. Physiol.* 517, 159–180.
- Loewenstein, W.R., 1981. Junctional intercellular communication: the cell-to-cell membrane channel. *Physiol. Rev.* 61, 829–913.
- Loiselle, F.B., Morgan, P.E., Alvarez, B.V., Casey, J.R., 2004. Regulation of the human NBC3  $\text{Na}^+/\text{HCO}_3^-$  co-transporter by carbonic anhydrase II and PKA. *Am. J. Physiol.* 286, C1423–C1433.
- Noma, A., Tsuboi, N., 1987. Dependence of junctional conductance on proton, calcium and magnesium ions in cardiac paired cells of guinea-pig. *J. Physiol.* 382, 193–211.
- O'Dowd, J.J., Robins, D.J., Miller, D.J., 1988. Detection, characterisation, and quantification of carnosine and other histidyl derivatives in cardiac and skeletal muscle. *Biochim. Biophys. Acta* 967 (2), 241–249.
- Orchard, C.H., Cingolani, H.E., 1994. Acidosis and arrhythmias in cardiac muscle. *Cardiovasc. Res.* 28 (9), 1312–1319.
- Orchard, C.H., Kentish, J.C., 1990. Effects of changes of pH on the contractile function of cardiac muscle. *Am. J. Physiol.* 258, C967–C981.
- Pelloux, S., Robillard, J., Ferrera, R., et al., 2005. Non beating HL-1 cells for confocal microscopy. Application to mitochondrial functions during cardiac preconditioning. *Prog. Biophys. Mol. Biol.* 89.
- Petrecchia, K., Atanasiu, R., Grinstein, S., Orłowski, J., Shrier, A., 1999. Subcellular localisation of the  $\text{Na}^+/\text{H}^+$  exchanger NHE1 in the rat myocardium. *Am. J. Physiol.* 276, H709–H717.
- Poole, R.C., Halestrap, A.P., Price, S.J., Levi, A.J., 1989. The kinetics of transport of lactate and pyruvate into isolated cardiac myocytes from guinea pig. Kinetic evidence for the presence of a carrier distinct from that in erythrocytes and hepatocytes. *Biochem. J.* 264 (2), 409–418.
- Sender, S., Decker, B., Fenske, C.D., Sly, W.S., Carter, N.D., Gros, G., 1998. Localisation of carbonic anhydrase IV in rat and human heart muscle. *J. Histochem. Cytochem.* 46, 855–861.
- Spitzer, K.W., Ershler, P.R., Skolnick, R.L., Vaughan-Jones, R.D., 2000. Generation of intracellular pH gradients in single cardiac myocytes with a microperfusion system. *Am. J. Physiol.* 278 (4), H1371–H1382.
- Spitzer, K.W., Skolnick, R.L., Percy, B.E., Keener, J.P., Vaughan-Jones, R.D., 2002. Facilitation of intracellular  $\text{H}^+$  ion mobility by  $\text{CO}_2/\text{HCO}_3^-$  in rabbit ventricular myocytes is regulated by carbonic anhydrase. *J. Physiol.* 541 (1), 159–167.
- Spray, D.C., Harris, A.L., Bennett, M.V., 1981. Gap junctional conductance is a simple and selective function of intracellular pH. *Science* 211, 712–715.
- Sterling, D., Alvarez, B.V., Casey, J.R., 2002. The extracellular component of a transport metabolon. Extracellular loop 4 of the human AE1  $\text{Cl}^-/\text{HCO}_3^-$  exchanger binds carbonic anhydrase IV. *J. Biol. Chem.* 277 (28), 25239–25246.

- Stewart, A.K., Boyd, C.A.R., Vaughan-Jones, R.D., 1999. A novel role for carbonic anhydrase: pH gradient dissipation in mouse small intestinal enterocytes. *J. Physiol.* 516, 209–217.
- Stewart, A.K., Kerr, N., Chernova, M.N., Alper, S.L., Vaughan-Jones, R.D., 2004. Acute pH-dependent regulation of AE2-mediated anion exchange involves discrete local surfaces of the NH<sub>2</sub>-terminal cytoplasmic domain. *J. Biol. Chem.* 279 (50), 52664–52676.
- Swietach, P., Vaughan-Jones, R.D., 2004. Novel method for measuring junctional proton permeation in isolated ventricular myocyte cell pairs. *Am. J. Physiol.* 287 (5), H2352–H2363.
- Swietach, P., Vaughan-Jones, R.D., 2005a. Spatial regulation of intracellular pH in the ventricular myocytes. *NY Acad. Sci. Ann.* 1047, 271–282.
- Swietach, P., Vaughan-Jones, R.D., 2005b. Relationship between intracellular pH and proton mobility in rat and guinea-pig ventricular myocytes. *J. Physiol.* 566 (3), 793–806.
- Swietach, P., Zaniboni, M., Stewart, A.K., Rossini, A., Spitzer, K.W., Vaughan-Jones, R.D., 2003. Modelling intracellular H<sup>+</sup> ion diffusion. *Prog. Biophys. Mol. Biol.* 83 (2), 69–100.
- Swietach, P., Leem, C.H., Spitzer, K.W., Vaughan-Jones, R.D., 2005a. Experimental generation and computational modeling of intracellular pH gradients in cardiac myocytes. *Biophys. J.* 88 (4), 3018–3037.
- Swietach, P., Spitzer, K.W., Vaughan-Jones, R.D., 2005b. Local release of caged protons by UV flash photolysis as a means of producing intracellular pH non-uniformity. *FASEB J.* 19, A146.
- Taegtmeier, H., 1978. Metabolic responses to cardiac hypoxia. Increased production of succinate by rabbit papillary muscles. *Circ. Res.* 43 (5), 808–815.
- Tanaka, H., Oyamada, M., Tsujii, E., Nakajo, T., Takamatsu, T., 2002. Excitation-dependent intracellular Ca<sup>2+</sup> waves at the border zone of the cryo-injured rat heart revealed by real-time confocal microscopy. *J. Mol. Cell. Cardiol.* 34, 1501–1512.
- Tsujii, E., Tanaka, H., Oyamada, M., Fujita, K., Hamamoto, T., Takamatsu, T., 2003. In situ visualisation of intracellular Ca<sup>2+</sup> dynamics at the border of the acute myocardial infarct. *Mol. Cell. Biochem.* 248, 135–139.
- Valiunas, V., Beyers, E.C., Brink, P.R., 2002. Cardiac gap junction channels show quantitative differences in selectivity. *Circ. Res.* 91, 104–111.
- Vandenberg, J.I., Carter, N.D., Bethell, H.W., Nogradi, A., Ridderstrale, Y., Metcalfe, J.C., Grace, A.A., 1996. Carbonic anhydrase and cardiac pH regulation. *Am. J. Physiol.* 271 (6), C1838–C1846.
- Vanysek, P., 1999. Ionic conductivity and diffusion at infinite dilution. In: Linde, D.R. (Ed.), *CRC Handbook of Chemistry and Physics*, 79th ed. Section 5 Thermochemistry, Electrochemistry and Kinetics. CRC Press, London, pp. 93–95.
- Vaughan-Jones, R.D., Lederer, W.J., Eisner, D.A., 1983. Ca<sup>2+</sup> ions can affect intracellular pH in mammalian cardiac muscle. *Nature* 301 (5900), 522–524.
- Vaughan-Jones, R.D., Peercy, B.E., Keener, J.P., Spitzer, K.W., 2002. Intrinsic H<sup>+</sup> mobility in the rabbit ventricular myocyte. *J. Physiol.* 541, 139–158.
- White, R.L., Doeller, J.F., Verselis, V.K., Wittenberg, B.A., 1990. Gap junctional conductance between cell-pairs of ventricular myocytes is modulated synergistically by H<sup>+</sup> and Ca<sup>2+</sup>. *J. Gen. Physiol.* 95, 1061–1075.
- Wilensky, R.L., Tranum-Jensen, J., Coronel, R., Wilde, A.A., Fiolet, J.W., Janse, M.J., 1986. The subendocardial border zone during acute ischemia of the rabbit heart: an electrophysiologic, metabolic, and morphologic correlative study. *Circulation* 74 (5), 1137–1146.
- Yamamoto, T., Swietach, P., Rossini, A., Loh, S.H., Vaughan-Jones, R.D., Spitzer, K.W., 2005. Functional diversity of electrogenic Na<sup>+</sup>–HCO<sub>3</sub><sup>–</sup> cotransport in ventricular myocytes from rat, rabbit and guinea-pig. *J. Physiol.* 562, 455–475.
- Yeager, M., 2000. Molecular biology and structure of cardiac gap junction intercellular channels. In: Zipes, D.P., Jalife, J.J. (Eds.), *Cardiac Electrophysiology, From Cell to Bedside*. WB Saunders, London (Chapter 4).
- Zaniboni, M., Rossini, A., Swietach, P., Banger, N., Spitzer, K.W., Vaughan-Jones, R.D., 2003a. Proton permeation through the myocardial gap junction. *Circ. Res.* 93, 726–735.
- Zaniboni, M., Swietach, P., Rossini, A., Yamamoto, T., Spitzer, K.W., Vaughan-Jones, R.D., 2003b. Intracellular proton mobility and buffering power in cardiac ventricular myocytes from rat, rabbit, and guinea pig. *Am. J. Physiol.* 285 (3), H1236–H1246.